ARCHIVES OF ORAL BIOLOGY 58 (2013) 181–191

Available online at www.sciencedirect.com

SciVerse ScienceDirect

journal homepage: http://www.elsevier.com/locate/aob

Expression and localization of receptor protein tyrosine phosphatase β and its ligand pleiotrophin in the submandibular gland of mice

Kannika Adthapanyawanich, Miyuki Yamamoto, Tomohiko Wakayama, Hiroki Nakata, Sunisa Keattikunpairoj, Shoichi Iseki *

Department of Histology and Embryology, Graduate School of Medical Science, Kanazawa University, Kanazawa, Ishikawa 920-8640, Japan

ARTICLE INFO

Article history:
Accepted 20 September 2012

Keywords:
RPTPβ
Pleiotrophin
Salivary gland
Duct system
Sexual dimorphism
Androgens
Mouse

ABSTRACT

Objectives: The family of receptor protein tyrosine phosphatase β (RPTPβ) is composed of 4 splice variants and thought to play roles in the neural migration and outgrowth. Several ligands including the growth factor pleiotrophin (PTN) bind to RPTPβ and inhibit its phosphatase activity, thereby activating cellular signalling pathways. We examined the expression and localization of RPTPβ and its ligands in the submandibular gland (SMG) of mice, which is known for a prominent sexual dimorphism in the duct system.

Design: The homogenates and tissue sections of male and female mouse SMG were analysed with RT-PCR, Western blotting, and immunohistochemistry.

Results: The short receptor type of RPTPβ (RPTPβ-S) was dominantly expressed in the SMG, and the male gland had significantly higher levels of RPTPβ-S expression than the female gland. In the male, RPTPβ-S was localized predominantly in intercalated duct (ID) cells, but was not found in granular convoluted tubule (GCT) cells or acinar cells. In the female, weaker reactivity was demonstrated in both ID and striated duct (SD) cells. Of the known ligands for RPTPβ, PTN was expressed in the SMG, without sexual difference in levels. In the male, PTN was localized in ID cells as well as in cells located in the distal ends of GCT that are in close vicinity to the ID, whereas in the female PTN was colocalized with RPTPβ-S throughout ID and SD cells.

Conclusions: These results indicated that the distribution of RPTPβ-S and its ligand PTN has a close relation to the sexual dimorphism in the duct system of mouse SMG.

1. Introduction

The submandibular gland (SMG) of rodents is composed of the acinus and the duct system, the latter composed of the intercalated duct (ID), striated duct (SD), granular convoluted tubule (GCT), and excretory duct.[1] Extensive development of the GCT from the SD takes place postnatally around the puberty in an androgen-dependent manner, resulting in a marked sexual dimorphism in the morphology and function of the duct system, with the GCT developed preferentially in the male gland.[2–4] The epithelial cells of GCT have abundant secretory granules that contain a variety of biologically active peptides such as nerve growth factor (NGF) and epidermal

* *Corresponding author*. Tel.: +81 76 265 2150; fax: +81 76 234 4220.
E-mail address: siseki@med.kanazawa-u.ac.jp (S. Iseki).

Abbreviations: SMG, submandibular gland; SLG, sublingual gland; ID, intercalated duct; SD, striated duct; GCT, granular convoluted tubule; RPTPβ, receptor protein tyrosine phosphatase β; PTN, pleiotrophin; NGF, nerve growth factor; IHC, immunohistochemistry.

0003–9969/$ – see front matter
http://dx.doi.org/10.1016/j.archoralbio.2012.09.005

growth factor (EGF).[5] Castration of males causes involution of the GCT accompanied by conversion of the phenotype of GCT cells into that of SD cells, whereas administration of androgens to females or castrated males causes the opposite phenomenon.[6,7] Such androgen-dependent GCT differentiation is accompanied by upregulation of the gene expression for GCT-specific products,[8] but the molecular mechanism underlying this differentiation is largely unknown.

The receptor protein tyrosine phosphatase β (RPTPβ), also known as protein tyrosine phosphatase ζ (PTPζ), was originally found in the central nervous system.[9,10] RPTPβ forms a family consisting of 4 splice variants, i.e., the long and short transmembrane receptor proteins (RPTPβ-L and -S, respectively), and the long and short secretory proteins (phosphacan and phosphacan short isoform, respectively).[11–13] In the receptor types of RPTPβ, the extracellular proteoglycan domains bind to multiple ligands, and the intracellular tyrosine-phosphatase domains de-phosphorylate various substrates, resulting in the regulation of cellular signalling pathways.[10] The members of the RPTPβ family are mainly expressed in neurons and glia of the embryonic and adult central nervous system and thought to be involved in the neural differentiation and migration, neurite outgrowth, synaptic formation and regulation.[10,14–16] Several molecules including the growth factor pleiotrophin (PTN) have been known as ligands for RPTPβ.[17–20] Upon binding of the ligands, RPTPβ forms homodimers and looses its tyrosine phosphatase activity, resulting in activation by phosphorylation of cellular signalling molecules.[21,22]

In a preliminary study analysing transcripts from the male and female mouse SMG with a DNA microarray, we found RPTPβ to be expressed more abundantly in the male than female gland (data not shown). Therefore, in the present study we examined the expression and localization of the members of the RPTPβ family and its ligands in the mouse SMG, with special reference to its sexual dimorphism.

2. Materials and methods

2.1. Animals and organs

Male and female Slc:ddY mice at the age of 8 weeks (W), some of which underwent testectomy at 6W, were purchased from Nippon SLC (Hamamatsu, Japan), reared under standard 12 h light/12 h dark laboratory conditions with free access to standard food and water, and used at the ages of 8–10W (adults). Mice at the ages of 2W and 5W were also used. All subsequent experiments were conducted in accordance with the Guidelines for the Care and Use of Laboratory Animals at Kanazawa University. Some female and testectomized male adults were subjected to subcutaneous injections of 25 mg/kg testosterone (Wako Pure Chemical Industries, Osaka, Japan) dissolved in 0.1 ml of olive oil every 24 h, and used either at 6 h after a single injection or at 6 h after 5 consecutive injections. Groups of 6–9 male and female animals in various ages and experimental conditions were sacrificed under pentobarbital anaesthesia by transcardial perfusion with physiological saline. For RT-PCR and Western blot analyses, the SMG, sublingual gland (SLG), parotid gland, extraorbital lacrimal gland, and cerebrum (subsequently referred to as brain) were dissected out, frozen immediately in liquid nitrogen, and stored at −80 °C until use. For immunohistochemical (IHC) analysis, the animals were fixed by perfusion with 4% paraformaldehyde in 0.1 M phosphate buffer, pH 7.2, the SMG was dissected out, and further fixed by immersion in the same fixative overnight at 4 °C. The specimens were then either rinsed overnight at 4 °C with 30% sucrose in 0.1 M phosphate buffer, frozen, and cut into 8 μm sections using a cryostat, or dehydrated in a graded ethanol series, embedded in paraffin, and cut into 4 μm sections using microtome. The cryostat and paraffin sections were mounted on silanized glass slides (DAKO, Glostrup, Denmark).

2.2. RNA preparation and conventional RT-PCR

Total RNA was isolated from the frozen specimens with the guanidinine-phenol-chloroform method using a commercial solution (TRI reagent; Sigma–Aldrich Co., St. Louis, MO). The first-strand cDNA was synthesized from 2 μg-aliquot of the total RNA samples using the oligo(dT)20 primer and Moloney murine leukaemia virus reverse transcriptase (Toyobo, Osaka, Japan). From these RT products, cDNA fragments for RPTPβ family members and other proteins were amplified with conventional and quantitative PCR. The sequences of the primer pairs used in the present study are listed in Table 1. The primer pairs for the RPTPβ family are either those common to all the members or those capable of distinguishing each member specifically. The sequences of the specific primer pairs were designed according to the genomic sequence of RPTPβ (NCBI Reference, NC_000072) using the SpliceMiner tool, taking advantage of that the family members are derived from differential splicing in the Exon12. The conventional RT-PCR was first performed for 30 cycles using TaqDNA polymerase (ExTaq; Takara Biomedicals, Kusatsu, Japan) in a DNA thermal cycler (MJ Research, Watertown, MA), and the amplified products were analysed with an agarose-gel electrophoresis.

2.3. Real-time quantitative RT-PCR

The real-time quantitative RT-PCR was performed in a Stratagene Mx-3005P Thermocycler (Stratagene, La Jolla, CA) according to the procedures recommended by the manufacturer. LightCycler DNA Master SYBR Green I (Roche Diagnostics, Indianapolis, IN) was used to detect the amplification of cDNA in a total volume of 20 μl with the absolute quantitative, ΔCt method.[23] Each reaction consisted of 10 μl of SYBR green I, 1 μl of the cDNA sample, 0.5 μl of each primer pair (10 pmol/μl), and 8 μl of distilled water. Thermal cycling conditions were 10 min at 95 °C followed by 45 cycles at 95 °C for 40 s, 60 °C for 30 s, and 72 °C for 30 s. GAPDH was employed as the endogenous control to normalize the data. Each sample was analysed in triplicates, and samples from 3 different animals were analysed to determine each value.

2.4. Preparation of primary antibodies

Rabbit polyclonal anti-PTN antibody and anti-NGF antibody were purchased from Santa Cruz Biotechnology (Santa Cruz,

Table 1 – Specific primers used for RT-PCR analysis.

Gene	GenBank	Fraction length (bp)	Primer direction	Sequence
RPTPβ[a]	NM_001081306	150	Forward	5′-ACCAGCCTTCTGGTCACATG-3′
			Reverse	5′-GAGAATGGCACCCAAGTCCT-3′
RPTPβ-L	BC151071	153	Forward	5′-ACCATCTGTTACTAGTGGGC-3′
			Reverse	5′-AAAGTCAGGGCAGACACGAT-3′
RPTPβ-S	BC157965	155	Forward	5′-ACCGAAGTGACACCACAGGC-3′
			Reverse	5′-TCCAACCCCTCAGCTAGACC-3′
Phosphacan[b]	AJ133130	154	Forward	5′-GGTCCTCCACACCATCTGTT-3′
			Reverse	5′-GACCGGAATTCCTTTCTTCC-3′
GAPDH	NM_008084	579	Forward	5′-AAGGGCTCATGACCACAGTC-3′
			Reverse	5′-AGGGAGATGCTCAGTGTTGG-3′
		151	Forward	5′-CATGGCCTTCCGTGTTCCTA-3′
			Reverse	5′-CTGGTCCTCAGTGTAGCCCAA-3′
PTN[c]	NM_008973	470	Forward	5′-ATGTCGTCCCAGCAATATCA-3′
			Reverse	5′-TTCTTCTTCTTTGACTCCGC-3′
Midkine	NM_010784	153	Forward	5′-ACCCACCAGTGCCTTTTGTC-3′
			Reverse	5′-TAACAAGTATCAGGGTGGGG-3′
Tenastin	NM_011607	530	Forward	5′-TGCAACGAGCCCCTTTGCCT-3′
			Reverse	5′-ATGCACTTGCCCTGTACGCA-3′
Contactin	NM_001159647	501	Forward	5′-CATTGCTGGTCAGCCATCTC-3′
			Reverse	5′-GGTAGCTAAGATCATCTGGG-3′
N-CAM	NM_001081445	350	Forward	5′-ACCGGAAATCAGGCTCCCAT-3′
			Reverse	5′-CCTCCATGTCTTTGCCCTTG-3′
NFP[d]	NM_010904	151	Forward	5′-TGCCCTCACCAAACAGGAAT-3′
			Reverse	5′-GCGTAGCGTTCAGCATACAT-3′

[a] RPTP-β: the primer pair is common to all 4 types of the RPTP-β family.
[b] Phosphacan: the primer pair is common to phosphacan and phosphacan short isoform.
[c] PTN: pleiotrophin.
[d] NFP: the heavy chain of neurophilament protein.

CA), and mouse monoclonal anti-α-tubulin antibody was purchased from Sigma (St. Louis, MO). Rat polyclonal antisera against the cytoplasmic domain of RPTPβ-S (common with that of RPTPβ-L) were produced in our laboratory according to the method described previously.[24,25] Briefly, a recombinant oligopeptide 41 amino acids in length corresponding to the C-terminus of RPTPβ-S, that was fused with the carrier protein glutathione-s-transferase, was produced in bacteria BL21 (Novagen, Madison, WI) by introducing the expression vector pGEX-6p-1 (Amersham Pharmacia Biotech, Uppsala, Sweden). The oligopeptide was then emulsified with Freund's complete adjuvant and injected as antigen into footpads of adult female Wistar rats. A booster immunization was made 2 weeks later, and the antisera were collected 1 week after the booster.

2.5. *Western blotting*

Frozen SMG tissues were homogenized in a lysis buffer containing 50 mM Tris–HCl (pH 7.5), 150 mM NaCl, 1% NP-40, 0.5% sodium deoxycholate, 0.1%SDS, protease inhibitor cocktail (Complete™; Roche Diagnostics) and phosphatase inhibitor cocktail (PhosStop™; Roche Diagnostics). The tissue homogenates were then separated on 12% SDS-polyacrylamide gels and transferred to PVDF membranes (BioRad Laboratories, Hercules, CA). After being blocked with 5% non-fat skimmed milk in PBS, the membranes were incubated with rat anti-RPTPβ-S antisera (1:500 dilution), rabbit anti-PTN antibody (1:2000), or mouse anti-α-tubulin antibody (1:10,000 dilution) overnight at 4 °C. After being washed, the membranes were incubated with horseradish peroxidase-conjugated secondary antibody against rat, rabbit, or mouse IgG (1:2000) (Dako) for 1 h. The immunoreaction was detected and its intensity was quantified in ImageQuant LAS-4000 mini (Fujifilm Medical, Tokyo, Japan) after treatment of the blots with the chemiluminescent reagent ECL-plus (Amersham Pharmacia Biotech). Samples from 3 different animals were analysed to determine each value, and the relative intensity of RPTPβ-S bands against the corresponding α-tubulin bands were calculated.

2.6. *IHC*

Paraffin sections of SMG, 5 μm thick, were made with a microtome and mounted on silanized glass slides (Dako). After being deparaffinized in xylen and rehydrated in a graded ethanol series, the sections were pre-treated with 5% normal swine sera for 30 min. For IHC by the enzyme-detection method, the sections were incubated overnight at 4 °C with rat anti-RPTPβ-S antisera (1:200 dilution), rabbit anti-PTN antibody (1:1000 dilution), or rabbit anti-NGF antibody (1:400 dilution). To confirm specificity of the immunoreaction, the primary antibodies were replaced with non-immune rat or rabbit sera with the corresponding dilutions. After a wash with PBS, the sites of immunoreaction were visualized by incubating the sections successively with biotinylated anti-rat or anti-rabbit IgG antibody (Vector Laboratories, Burlingame, CA) at 1:200 for 1 h, horseradish peroxidase-conjugated streptavidin (Dako) at 1:300 for 1 h, and a peroxidase substrate (ImmPACT™ DAB, Vector Laboratories) for about 5 min. The sections were subjected to observation under an Olympus BX50 microscope. The pre-embedding immunoelectron microscopy was performed as described previously.[25] The

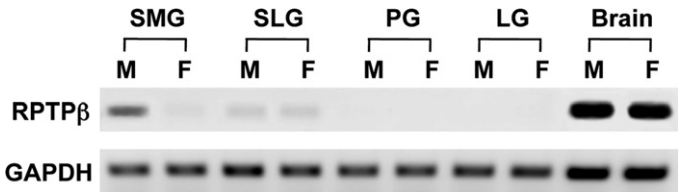

Fig. 1 – RT-PCR analysis for the expression of RPTPβ in the submandibular gland (SMG), sublingual gland (SLG), parotid gland (PG), extraorbitary lacrimal gland (LG) and cerebrum (Brain) of male (M) and female (F) adult mice. The products of amplification using the primer pair common to all 4 types of the RPTPβ family were electrophoresed and stained with ethidium bromide. Expression of GAPDH is shown as positive control.

cryostat sections of SMG immunostained with anti-RPTPβ-S antisera or anti-PTN antibody were fixed with 1% OsO_4, stained with 1% uranyl acetate and embedded in Glicidether (Selva Feinbiochemica, Heidelberg, Germany). Ultrathin sections were prepared using an ultramicrotome and subjected to observation with a JEM-1210 electron microscope (JEOL, Tokyo, Japan). For fluorescent double-immunostaining, the pretreated sections were incubated with rat anti-RPTPβ-S antisera (1:200) mixed with rabbit anti-PTN antibody (1:500) overnight at 4 °C. After being washed, the sections were incubated with a mixture of anti-rat IgG antibody conjugated with Alexa Fluor 594 and anti-rabbit IgG antibody conjugated with Alexa Fluor 488 (Molecular Probes, Eugene, OR) for 1 h. They were then mounted in glycerol and subjected to observation with an Olympus BX50/BX-FLA fluorescent microscope. The IHC results were confirmed in the SMG from 3 different animals.

2.7. *Statistical analysis*

The statistical difference was analysed between two values with Student's *t*-test, and among multiple values with one-factor analysis of variance (ANOVA) followed by Bonferroni's post hoc test. The difference with a *P* value less than 0.05 was considered significant.

3. Results

3.1. *Expression of the RPTPβ family in salivary and lacrimal glands*

In the RT-PCR analysis (30 cycles) using the primers common to all 4 types of RPTPβ, expression of the mRNA for RPTPβ was detected abundantly in the SMG as well as in the brain, and slightly in SLG, but was not detected in the parotid or lacrimal gland. In the SMG, the expression appeared substantially stronger in the male gland than the female gland (Fig. 1). Such sexual difference was not recognized in the brain or SLG.

3.2. *Expression of different types of RPTPβ in the male and female SMG*

Of the 4 types of RPTPβ, only the short receptor type (RPTPβ-S) was abundantly expressed in the SMG with the RT-PCR analysis (30 cycles) using the specific primer pairs, but the transcripts for long receptor type (RPTPβ-L) or long and short secretory types (phosphacan and phosphacan short isoform) were not or scarcely detected (Fig. 2A). The expression of RPTPβ-S in the SMG appeared much more abundant in the male than female. These results were further confirmed in the real-time quantitative RT-PCR (Fig. 2B). When compared for the copy numbers normalized with those of GAPDH, the abundance of RPTPβ-S mRNA in the male SMG was 45% that in

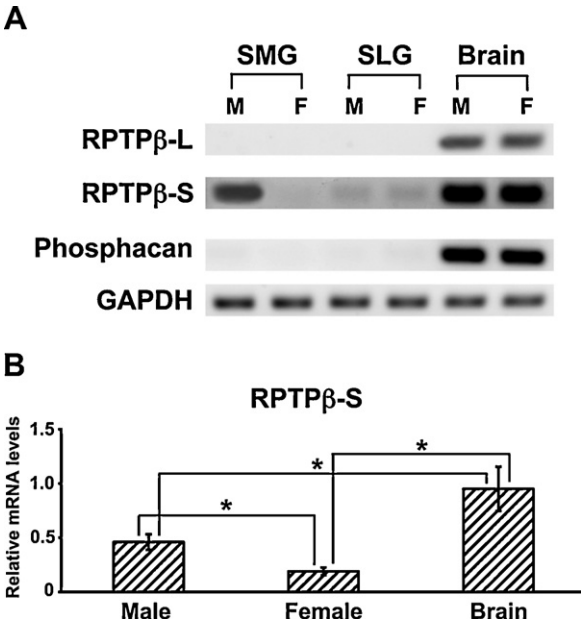

Fig. 2 – (A) Conventional RT-PCR analysis for the expression of RPTPβ-L, RPTPβ-S, and phosphacan in the SMG, SLG, and brain of male (M) and female (F) adult mice. The products of amplification using primer pairs specific to each type of RPTPβ were electrophoresed and stained with ethidium bromide. The primer pair for phosphacan is common to phosphacan and phosphacan short isoform. Expression of GAPDH is shown as positive control. (B) Real-time quantitative RT-PCR analysis for the expression of RPTPβ-S in the male and female SMG and male brain. The levels of mRNA for each type of RPTPβ were normalized by dividing with those for GAPDH. The value in the brain was set as 1.0 and the relative values in the male and female SMG are indicated. Each value represents mean ± SD of 3 animals. *Significantly different ($P < 0.05$).

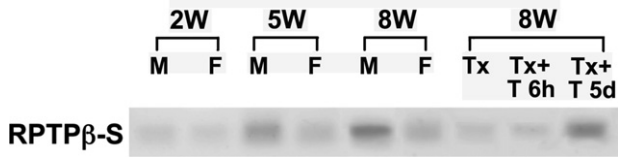

Fig. 3 – RT-PCR analysis for the effects of sex, postnatal days and hormonal conditions on the expression of RPTPβ-S in the SMG. The products of amplification in SMG from male (M) and female (F) mice at 2W, 5W and 8W (adult) postpartum, and from testectomized adult male mice (Tx), Tx at 6 h and 5 days after single and repeated administrations of testosterone (T), respectively, were electrophoresed and stained with ethydium bromide.

the brain and 2.2-fold that in the female SMG (significantly different, $P < 0.05$).

3.3. *Androgen dependency of the expression of RPTPβ-S in the SMG*

The levels of expression of RPTPβ-S in the SMG had no sexual difference at 2 weeks postpartum, but were elevated continuously in the male at 5 and 8 weeks, coincident with known postnatal development of the GCT in the male gland (Fig. 3). Upon testectomy, the levels of RPTPβ-S in the male gland decreased to those in the normal female gland. Single administration of testosterone to testectomized males had no effect after 6 h, but repeated administration of testosterone for 5 days restored the levels of the normal male gland. Administration of testosterone to females caused the same effect as in testectomized males (data not shown). Androgen-dependent differentiation of the duct system, as represented by the preferential development of GCT cells in the male gland and testosterone-treated female or testectomized male gland, was verified with immunostaining for NGF, a specific marker of GCT cells (Fig. 4).

3.4. *Expression of RPTPβ-S protein in the SMG*

With Western blotting using the specific rat antisera against the cytoplasmic domain common to the receptor types of RPTPβ, the band of 220 kDa corresponding to RPTPβ-S was detected in the SMG, with 1.8-fold higher intensity in the male than female (significantly different, $P < 0.05$) (Fig. 5). In contrast, the band of 380 kDa corresponding to RPTPβ-L was detected in the brain but not in the SMG. The reason why the band for RPTPβ-S was scarcely detected in the brain is unclear, but the brain (cerebrum) may indeed produce much smaller amount of RPTPβ-S than RPTPβ-L at the protein level.

3.5. *Immunohistochemical localization of RPTPβ-S protein in the SMG*

The male and female SMG were examined with IHC for RPTPβ-S. In the male gland, intense immunoreactivity was localized predominantly in ID, whereas the rest of the intralobular duct portions, composed mostly of GCT, were completely immunonegative (Fig. 6A and B). Large extralobular ducts (excretory ducts) were weakly immunostained. In contrast, in the female gland, where GCT cells are scarce, immunoreactivity of moderate intensity was distributed throughout the intralobular duct portions composed of ID and SD. The acini showed no immunostaining in either sex. IHC with the primary antibody replaced by non-immune rat sera showed no immunostaining (data not shown). With electron microscopic IHC, intense immuoreactivity in the male gland was recognized throughout the membrane and cytoplasmic portions of ID cells, thus it was difficult to determine if the reactivity was stronger in the luminal or basal portions of the cell membrane (Fig. 6C and D). The patterns of the distribution of RPTPβ-S in the SMG of testectomized mice and testosterone-treated female or testectomized mice were essentially the same as in those of female and male mice, respectively (data not shown).

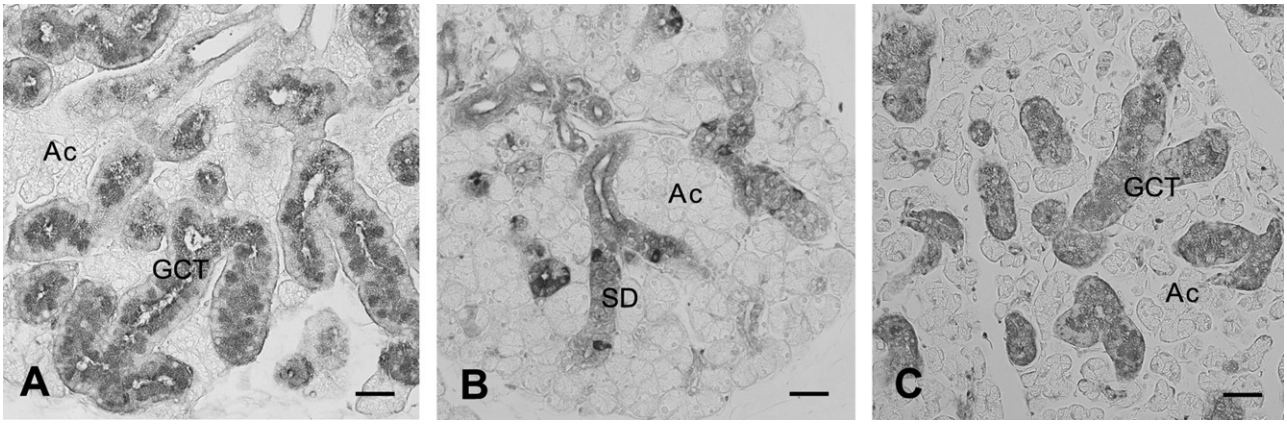

Fig. 4 – The sexual dimorphism and the effect of testosterone in the duct system of mouse SMG. SMG from adult male (A), female (B) and female mice treated with testosterone for 5 consecutive days (C) were immunostained with anti-NGF antibody. (A) and (C) The duct system is largely occupied with GCT cells (GCT) that have abundant NGF-positive secretory granules. (B) Only a small number of NGF-positive cells are scattered among SD cells (SD) that have low or no NGF-immunoreactivity. The results in the SMG of testectomized mice and testosterone-treated testectomized mice are essentially the same as B and C, respectively (data not shown). Ac, acinus. Bar = 40 μm.

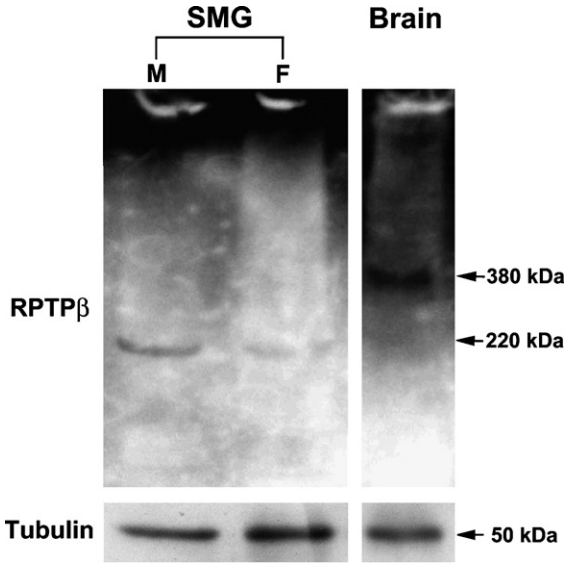

Fig. 5 – Western blot analysis for the expression of RPTPβ-S in the male (M) and female (F) SMG and male brain. The protein samples were electrophoresed, blotted and immunostained with rat anti-RPTPβ-S antisera. This antibody recognizes both RPTPβ-S and -L. The expression of α-tubulin is shown as loading control. The molecular weights (kDa) of the immunoreactive bands are indicated.

3.6. *Expression of the ligands of RPTPβ in the SMG*

Of the known ligands for the RPTPβ family tested (PTN, midkine, tenastin, contactin and N-CAM), only the growth factor PTN was abundantly expressed in the SMG, as detected with RT-PCT (30 cycles), without sexual difference in levels (Fig. 7). No mRNA for neurofilament protein, a specific marker of neurons, was detected in the SMG with the same amplification condition. This result, together with the absence of neuronal ganglion cells in the histological sections of SMG, suggests that the contribution of neuron-derived transcripts in SMG is negligible in the present study. With Western blotting using the specific rabbit antibody against PTN, the specific band of approximately 15 kDa was detected in the SMG, without sexual difference in intensity (Fig. 8).

3.7. *Immunohistochemical localization of PTN protein in the SMG*

With IHC, the distribution of PTN in the male and female SMG was also restricted to the duct system (Fig. 9A and B). In the male gland, the immunoreactivity was primarily present in ID cells but was also found in cells located in the distal ends of GCT that are adjacent to ID (In this paper, ''distal'' refers to a part of the duct system that is closer to the acinus). In contrast, in the female gland the immunoreactivity was present

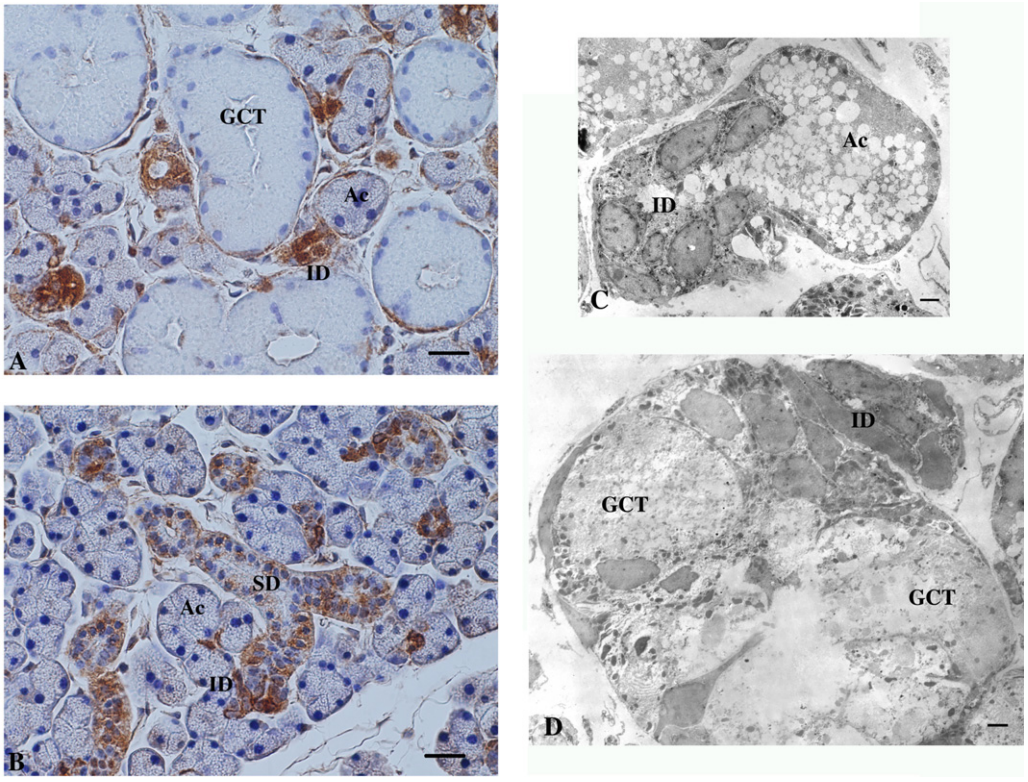

Fig. 6 – Immunohistochemical localization of RPTPβ-S. Paraffin sections of the male (A) and female (B) SMG were immunostained with anti-RPTPβ-S antisera and visualized with the enzyme-histochemical method. Ac: acinus; ID: intercalated duct; SD: striated duct; GCT: granular convoluted tubule. Bar = 20 μm. (C) and (D) A cryostat section of the male SMG was immunostained with anti-RPTPβ-S antisera and visualized with electron microscopy with the pre-embedding, enzyme-histochemical method. Note the dark immunoreaction products present in the entire portions of ID cells (ID) but absent in acinar cells (Ac) or GCT cells (GCT). Bars = 2 μm.

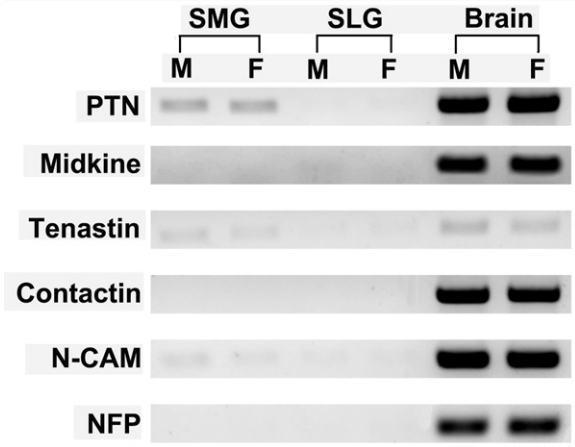

Fig. 7 – RT-PCR analysis for the expression of various ligands for RPTPβ-S in the SMG, SLG and brain. The products amplified with the primer pairs for pleiotrophin (PTN), midkine, tenastin, contactin and N-CAM were electrophoresed and stained with ethidium bromide. Expression of the heavy chain of neurofilament protein (NFP) is also shown as a specific marker of neurons.

diffusely in most ID and SD cells. With electron microscopic IHC, the intense immuoreactivity for PTN in the female gland was recognized in both membrane and cytoplasmic portions of SD cells, thus it was difficult to determine if the reactivity was stronger in the luminal or basal portions of the cytoplasm (Fig. 9C). Double-immunostaining confirmed that PTN-positive cells mostly overlap with RPTPβ-S-positive cells in the ID of both sexes and SD of the female, although PTN appeared weaker in the ID than SD, and RPTPβ-S appeared weaker in the proximal portions than the distal portions of SD (Fig. 10). In addition, cells in the distal ends of GCT of the male were positive for PTN but negative for RPTPβ-S.

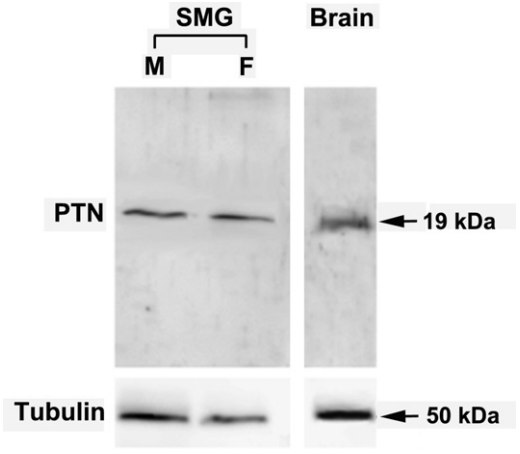

Fig. 8 – Western blot analysis for the expression of PTN in the male (M) and female (F) SMG and male brain. The protein samples were electrophoresed, blotted and immunostained with rat anti-PTN antibody. The expression of α-tubulin is shown as loading control. The molecular weights (kDa) of the immunoreactive bands are indicated.

4. Discussion

The cellular kinetics responsible for formation and maintenance of the structure of rodent SMG are not fully understood. In the first few postnatal weeks, cells constituting the distal ends of intralobular ducts (terminal tubules) give rise to acinar cells and undergo extensive proliferation, a process promoted by β-adrenergic mechanisms.[26–28] Thereafter the duct system continues to develop to form different compartments, of which the GCT is differentiated from the SD after puberty dependent on the action of hormones, mainly of androgens.[4,6,7] In the adulthood, the acinar cells as well as cells of the different compartments of the duct system all retain proliferative potential of varying degrees. For example, single administration of β-adrenergic agonists like isoproterenol causes a remarkable increase in the proliferation rate of entire acinar cells.[29,30] Nevertheless, there is evidence that the ID compartment of adult rodent SMG contains stem cells, which proliferate and eventually replenish all parenchymal cell types of the SMG.[31–34] Kinetic studies using radiolabeled DNA precursors have revealed that ID cells differentiate into both acinar and GCT cells that are located at the opposite ends of the ID.[31,33,35] Thus, GCT cells in adult SMG arise from self-proliferation and also from differentiation of ID cells. Although in the female gland GCT cells are mostly replaced by SD cells, cells located at the ends of the SD and adjacent to the ID often have secretory granules and are considered to represent the intermediate between SD and GCT cells.[3,35,36] Furthermore, administration of androgens into females causes extensive conversion of SD cells into GCT cells.[6,7] These phenomena lead us to a concept that there is a cell lineage in the duct system originating from stem cells in the ID compartment and terminating in GCT cells through the stage of SD cells.[32,37] Higher levels of plasma androgens in the male may promote progression of this cell lineage at the step from SD to GCT cells.

In the present study, we revealed that RPTPβ-S, the short receptor type of RPTPβ with the molecular weight 220 kDa, is abundantly expressed in the SMG of mice, at higher levels in the male than female. This difference was about 2.2-fold at the mRNA level and 1.8-fold at the protein level. IHC revealed that RPTPβ-S is primarily localized in the ID in both sexes, contrary to the expectation that it might be localized in the GCT that is much more developed in the male. Furthermore, whereas in the female RPTPβ-S was also expressed in the SD, in the male it was completely negative in the GCT. Taking into account the male-dominance of the total levels of RPTPβ-S expression, the levels of RPTPβ-S expression in the ID is considered to be much higher in the male than female. Testosterone-induced conversion of SD into GCT cells in the SMG of females or testectomized males was accompanied by an increased expression of RPTPβ-S, presumably in ID cells. The continuous presence of RPTPβ-S in the ID through to SD in the female, in contrast to the clear gap between the presence in the ID and absence in the GCT of RPTPβ-S in the male, suggests that expression of RPTPβ-S has a close relation to

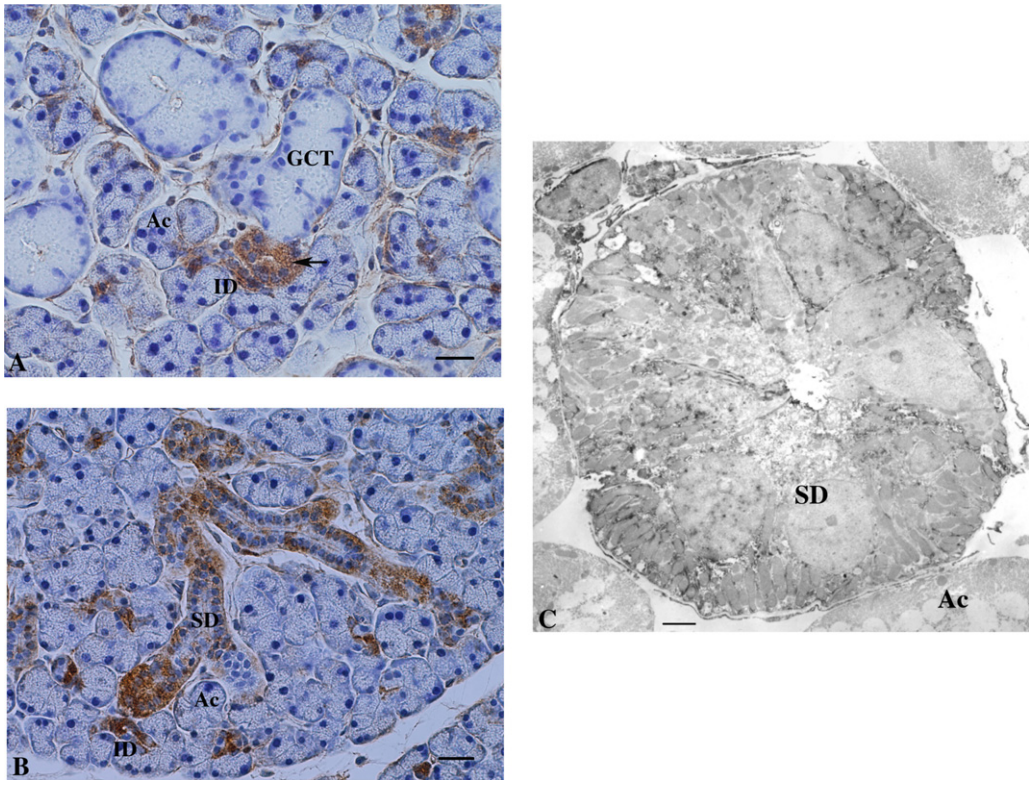

Fig. 9 – Immunohistochemical localization of PTN. Paraffin sections of the male (A) and female (B) SMG were immunostained with anti-PTN antibody and visualized with the enzyme-histochemical method. Ac: acinus; ID: intercalated duct; SD: striated duct; GCT: granular convoluted tubule. Note the positive immunoreaction in the distal end portions of GCT (arrow). Bar = 20 μm. (C) A cryostat section of the female SMG was immunostained with anti-PTN antibody and visualized in electron microscopy with the pre-embedding, enzyme-histochemical method. Note the dark immunoreaction products present in the entire portions of SD cells (SD) but absent in acinar cells (Ac). Bar = 2 μm.

androgen-dependent differentiation of the duct components leading to the sexual dimorphism.

The family of RPTPβ are expressed primarily in the central nervous system including the retina from the early embryonic ages through to adulthood, in both neurons and glia, suggesting pleiotrophic roles of RPTPβ in the neural differentiation and migration, neurite outgrowth, synaptic formation and regulation.[10,14–16] Although mice deficient for RPTPβ were initially described to display no obvious abnormality in the nervous system,[38] subsequent studies reported defects in myelination of oligodendrocytes[39] and abnormal motor coordination and nociception.[40] In addition to the nervous system, RPTPβ is known to be expressed in other organs and tissues, such as bone and stomach, and mice deficient for RPTPβ are reported to display abnormal bone remodeling[41] and resistance to gastric ulcer induction by *Helicobacter pylori* infection.[42] The biological significance of the presence of different types of RPTPβ is largely unknown. In the development of the central nervous system, including that of the retina, all types of RPTPβ seem to have similar biological roles.[43] Interestingly, similar to the present case, osteoblasts specifically express the short receptor type of RPTPβ (RPTPβ-S), the deficiency of which causes abnormality in bone remodelling in mice.[41]

Several ligands are known to bind to RPTPβ, including the extracellular matrix protein tenastin, the cell adhesion molecules contactin and N-CAM, and the growth factor PTN and midkine.[17–20] PTN is a 18 kDa secreted heparin-binding cytokine originally found in the uterus and brain.[44–46] PTN is expressed primarily in the neurons and glia in the embryonic and adult central nervous system,[47–49] in which it is thought to signal diverse functions, including neural stem cell differentiation, glial cell differentiatiation, neuronal migration, neurite outgrowth, and angiogenesis.[45,46,50,51] PTN is also expressed in a variety of developing non-neural tissues[47] and mitogenic for fibroblasts, endothelial, epithelial, and tumour cells.[50] Mice deficient for PTN display thickning of cerebral cortex and behavioural abnormality.[52,53] PTN was the first soluble molecule to be identified as ligand for RPTPβ.[19] Upon binding to the receptor, PTN inactivates the phosphatase activity of RPTPβ and thereby causes tyrosine phosphorylation of the substrates of RPTPβ such as β-catenin.[21] This may lead to activation of a variety of downstream signalling pathways. For example, PTN-induced loss of association of β-catenin with N-cadherin disrupts the cell-cell adhesion and causes epithelial-mesenchymal transition in cultured cells.[54]

In the present study, we revealed PTN to be expressed in the SMG without sexual difference in levels. PTN was

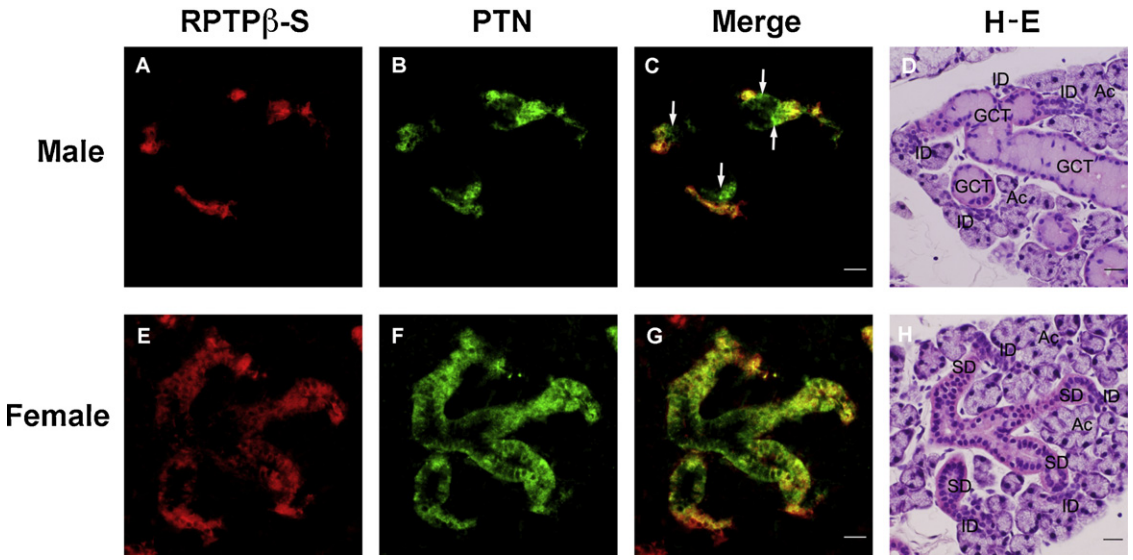

Fig. 10 – Double immunostaining for RPTPβ-S and PTN in the SMG. Paraffin sections of the male (A), (B) and(C) and female (E), (F) and (G) SMG were immunostained simultaneously with rat anti-RPTPβ-S antisera and rabbit anti-PTN antibody and observed with fluorescent microscopy. After washing, the same male (D) and female (H) SMG sections were stained with H-E. The fluorescence for RPTPβ-S (red; (A), (E) and PTN (green; (B), (F) overlaps to various extents in different portions of the duct system when merged (yellow; (C), (G). Note the single fluorescence for PTN in the distal end portions of GCT (arrows). Ac: acinus; ID: intercalated duct; SD: striated duct. Bar = 40 μm.

colocalized with RPTPβ-S in ID cells of both sexes and SD cells of the female. In addition, in the male PTN was present in cells in the distal ends of GCT that are negative for RPTPβ-S. Since the ultrastructural localization of RPTPβ-S to apical or basal membrane could not be determined in this study, the location of the ligand-receptor interaction is unknown. However, considering that the majority of ID and SD cells are lacking in apical secretory granules, the autocrine/paracrine mode of PTN binding to RPTPβ-S is likely operating at the basal membrane of these cell populations. On the other hand, there is evidence that RPTPβ-S of gastric epithelial cells can bind to *Helicobacter pylori* vacuolating cytotoxin that is secreted into the gastric lumen.[42] Therefore, a possibility is not ruled out that RPTPβ-S in the SMG is located in the apical membrane of duct epithelial cells and binds to some unknown ligand secreted into saliva.

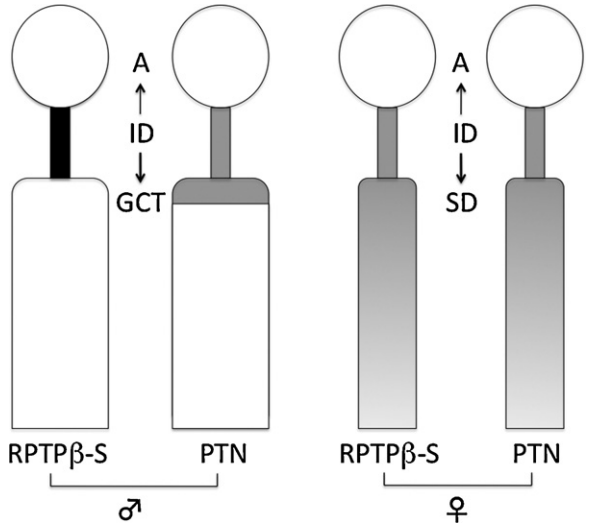

Fig. 11 – The distribution of RPTPβ-S and PTN and possible androgen-dependent progression of cell lineage in the male and female mouse SMG. A: acinus; ID: intercalated duct; GCT: granular convoluted tubule; SD: striated duct. Darkness of the mask in each duct portions represents intensity of the immunostaining.

The present study has revealed distinct patterns of expression of the receptor and ligand in the duct system of mouse SMG, i.e., presence of both RPTPβ-S and PTN in ID cells in both sexes and SD cells in the female, presence of PTN but absence of RPTPβ-S in a subpopulation of GCT cells adjacent to ID in the male, and absence of both PTN and RPTPβ-S in a majority of GCT cells in the male. These suggest that combinations of the presence or absence of RPTPβ-S or PTN are closely related to androgen-dependent progression of the cell lineage from ID to GCT cells (schematically presented in Fig. 11). Whether or not this is a causative relationship remains to be clarified in future study in terms of the molecular mechanisms underlying the duct cell differentiation in mouse SMG.

Funding

This study was supported in part by Grant-in-Aid for Scientific Research (No. 20590187 and 23590231) to SI from the Ministry

of Education, Culture, Sports, Science and Technology of Japan.

Competing interests

None declared.

Ethical approval

Ethical approval was not necessary for this work. The approval for the animal experiments was given by Kanazawa University (AP-081042 and AP-081043).

REFERENCES

1. Pinkstaff CA. The cytology of salivary glands. *International Review of Cytology* 1980;**63**:141–261.
2. Jacoby F, Leeson CR. The postnatal development of the rat submaxillary gland. *Journal of Anatomy* 1959;**93**(2):201–16.
3. Caramia F. Ultrastructure of mouse submaxillary gland. I. Sexual differences. *Journal of Ultrastructure Research* 1966;**16**(5):505–23.
4. Gresik EW. Postnatal developmental changes in submandibular glands of rats and mice. *Journal of Histochemistry and Cytochemistry* 1980;**28**(8):860–70.
5. Barka T. Biologically active polypeptides in submandibular glands. *Journal of Histochemistry and Cytochemistry* 1980;**28**(8):836–59.
6. Caramia F. Ultrastructure of mouse submaxillary gland. II. Effect of castration in the male. *Journal of Ultrastructure Research* 1966;**16**(5):524–36.
7. Chrétien M. Action of testosterone on the differentiation and secretory activity of a target organ: the submaxillary gland of the mouse. *International Review of Cytology* 1977;**50**:333–96.
8. Gubits RM, Shaw PA, Gresik EW, Onetti-Muda A, Barka T. Epidermal growth factor gene expression is regulated differently in mouse kidney and submandibular gland. *Endocrinology* 1986;**119**(3):1382–7.
9. Krueger NX, Saito H. A human transmembrane protein-tyrosine-phosphatase. PTP zeta, is expressed in brain and has an N-terminal receptor domain homologous to carbonic anhydrases. *Proceedings of the National Academy of Sciences of the United States of America* 1992;**89**(16):7417–21.
10. Levy JB, Canoll PD, Silvennoinen O, Barnea G, Morse B, Honegger AM, et al. The cloning of a receptor-type protein tyrosine phosphatase expressed in the central nervous system. *Journal of Biological Chemistry* 1993;**268**(14):10573–81.
11. Maurel P, Rauch U, Flad M, Margolis RK, Margolis RU. Phosphacan, a chondroitin sulfate proteoglycan of brain that interacts with neurons and neural cell-adhesion molecules, is an extracellular variant of a receptor-type protein tyrosine phosphatase. *Proceedings of the National Academy of Sciences of the United States of America* 1994;**91**(7):2512–6.
12. Nishiwaki T, Maeda N, Noda M. Characterization and developmental regulation of proteoglycan-type protein tyrosine phosphatase zeta/RPTPbeta isoforms. *Journal of Biochemistry* 1998;**123**(3):458–67.
13. Garwood J, Heck N, Reichardt F, Faissner A. Phosphacan short isoform, a novel non-proteoglycan variant of phosphacan/receptor protein tyrosine phosphatase-beta, interacts with neuronal receptors and promotes neurite outgrowth. *Journal of Biological Chemistry* 2003;**278**(26):24164–73.
14. Canoll PD, Barnea G, Levy JB, Sap J, Ehrlich M, Silvennoinen O, et al. The expression of a novel receptor-type tyrosine phosphatase suggests a role in morphogenesis and plasticity of the nervous system. *Brain Research Developmental Brain Research* 1993;**75**(2):293–8.
15. Engel M, Maurel P, Margolis RU, Margolis RK. Chondroitin sulfate proteoglycans in the developing central nervous system. I. cellular sites of synthesis of neurocan and phosphacan. *Journal of Comparative Neurology* 1996;**366**(1):34–43.
16. Maeda N, Noda M. Involvement of receptor-like protein tyrosine phosphatase zeta/RPTPbeta and its ligand pleiotrophin/heparin-binding growth-associated molecule (HB-GAM) in neuronal migration. *Journal of Cell Biology* 1998;**142**(1):203–16.
17. Milev P, Friedlander DR, Sakurai T, Karthikeyan L, Flad M, Margolis RK, et al. Interactions of the chondroitin sulfate proteoglycan phosphacan, the extracellular domain of a receptor-type protein tyrosine phosphatase, with neurons, glia, and neural cell adhesion molecules. *Journal of Cell Biology* 1994;**127**(6 Pt 1):1703–15.
18. Peles E, Nativ M, Campbell PL, Sakurai T, Martinez R, Lev S, et al. The carbonic anhydrase domain of receptor tyrosine phosphatase beta is a functional ligand for the axonal cell recognition molecule contactin. *Cell* 1995;**82**(2):251–60.
19. Maeda N, Nishiwaki T, Shintani T, Hamanaka H, Noda M. 6B4 proteoglycan/phosphacan, an extracellular variant of receptor-like protein-tyrosine phosphatase zeta/RPTPbeta, binds pleiotrophin/heparin-binding growth-associated molecule (HB-GAM). *Journal of Biological Chemistry* 1996;**271**(35):21446–52.
20. Maeda N, Ichihara-Tanaka K, Kimura T, Kadomatsu K, Muramatsu T, Noda M. A receptor-like protein-tyrosine phosphatase PTPzeta/RPTPbeta binds a heparin-binding growth factor midkine. Involvement of arginine 78 of midkine in the high affinity binding to PTPzeta. *Journal of Biological Chemistry* 1999;**274**(18):12474–9.
21. Meng K, Rodriguez-Peña A, Dimitrov T, Chen W, Yamin M, Noda M, et al. Pleiotrophin signals increased tyrosine phosphorylation of beta beta-catenin through inactivation of the intrinsic catalytic activity of the receptor-type protein tyrosine phosphatase beta/zeta. *Proceedings of the National Academy of Sciences of the United States of America* 2000;**97**(6):2603–8.
22. Pariser H, Perez-Pinera P, Ezquerra L, Herradon G, Deuel TF. Pleiotrophin stimulates tyrosine phosphorylation of β-adductin through inactivation of the transmembrane receptor protein tyrosine phosphatase β/ζ. *Biochemical and Biophysical Research Communications* 2005;**335**(1):232–9.
23. Schmittgen TD, Livak KJ. Analyzing real-time PCR data by the comparative C(T) method. *Nature Protocols* 2008;**3**:1101–8.
24. Wakayama T, Kato Y, Utsumi R, Tsuji A, Iseki S. A time- and cost-saving method of producing rat polyclonal antibodies. *Acta Histochemica et Cytochemica* 2006;**39**(3):79–87.
25. Wakayama T, Nakata H, Kurobo M, Sai Y, Iseki S. Expression, localization, and binding activity of the ezrin/radixin/moesin proteins in the mouse testis. *Journal of Histochemistry and Cytochemistry* 2009;**57**(4):351–62.
26. Chang WW, Barka T. Stimulation of acinar cell proliferation by isoproterenol in the postnatal rat submandibular gland. *Anatomical Record* 1974;**178**(2):203–9.
27. Cutler LS, Chaudhry AP. Cytodifferentiation of the acinar cells of the rat submandibular gland. *Developmental Biology* 1974;**41**(1):31–41.
28. Srinivasan R, Chang WW, van der Noen H, Barka T. The effect of isoproterenol on the postnatal differentiation and

growth of the rat submandibular gland. *Anatomical Record* 1973;**177**(2):243–53.
29. Barka T. Induced cell proliferation: the effect of isoproterenol. *Experimental Cell Research* 1965;**37**:662–79.
30. Baserga R, Heffler S. Stimulation of DNA synthesis by isoproterenol and its inhibition by actinomycin D. *Experimental Cell Research* 1967;**46**(3):571–80.
31. Zajicek G, Yagil C, Michaeli Y. The streaming submandibular gland. *Anatomical Record* 1985;**213**(2):150–8.
32. Denny PC, Denny PA. Dynamics of parenchymal cell division, differentiation, and apoptosis in the young female mouse submandibular gland. *Anatomical Record* 1999;**254**:408–17.
33. Man Y-G, Ball WD, Marchetti L, Hand A. Contributions of intercalated duct cells to the normal parenchyma of submandibular glands of adult rats. *Anatomical Record* 2001;**263**:202–14.
34. Kimoto M, Yura Y, Kishino M, Toyosawa S, Ogawa Y. Label-retaining cells in the rat submandibular gland. *Journal of Histochemistry and Cytochemistry* 2008;**56**(1):15–24.
35. Denny PC, Chai Y, Klauser DK, Denny PA. Parenchymal cellproliferation and mechanisms for maintenance of granular duct andacinar cell populations in adult male mouse submandibular gland. *Anatomical Record* 1993;**235**:475–85.
36. Chai Y, Klauser DK, Denny PA, Denny PC. Proliferative and structural differences between male and female mouse submandibular glands. *Anatomical Record* 1993;**235**(2):303–11.
37. Denny PC, Chai Y, Pimprapaiporn W, Denny PA. Three-dimensional reconstruction of adult female mouse submandibular gland secretory structures. *Anatomical Record* 1990;**226**(4):489–500.
38. Harroch S, Palmeri M, Rosenbluth J, Custer A, Okigaki M, Shrager P, et al. No obvious abnormality in mice deficient in receptor protein tyrosine phosphatase beta. *Molecular and Cellular Biology* 2000;**20**(20):7706–15.
39. Harroch S, Furtado GC, Brueck W, Rosenbluth J, Lafaille J, Chao M, et al. A critical role for the protein tyrosine phosphatase receptor type Z in functional recovery from demyelinating lesions. *Nature Genetics* 2002;**32**(3):411–4.
40. Lafont D, Adage T, Gréco B, Zaratin P. A novel role for receptor like protein tyrosine phosphatase zeta in modulation of sensorimotor responses to noxiousstimuli: evidences from knockout mice studies. *Behavioural Brain Research* 2009;**201**(1):29–40.
41. Schinke T, Gebauer M, Schilling AF, Lamprianou S, Priemel M, Mueldner C, et al. The protein tyrosine phosphatase Rptpzeta is expressed in differentiated osteoblasts and affects bone formation in mice. *Bone* 2008;**42**(3):524–34.
42. Fujikawa A, Shirasaka D, Yamamoto S, Ota H, Yahiro K, Fukada M, et al. Mice deficient in protein tyrosine phosphatase receptor type Z are resistant to gastric ulcer induction by VacA of *Helicobacter pylori*. *Nature Genetics* 2003;**33**(3):375–81.
43. Klausmeyer A, Garwood J, Faissner A. Differential expression of phosphacan/RPTPbeta isoforms in the developing mouse visual system. *Journal of Comparative Neurology* 2007;**504**(6):659–79.
44. Milner PG, Li YS, Hoffman RM, Kodner CM, Siegel NR, Deuel TF. A novel 17 kD heparin-binding growth factor (HBGF-8) in bovine uterus: purification and N-terminal amino acid sequence. *Biochemical and Biophysical Research Communications* 1989;**165**(3):1096–103.
45. Rauvala H. An 18-kd heparin-binding protein of developing brain that is distinct from fibroblast growth factors. *EMBO Journal* 1989;**8**(10):2933–41.
46. Li YS, Milner PG, Chauhan AK, Watson MA, Hoffman RM, Kodner CM, et al. Cloning and expression of a developmentally regulated protein that induces mitogenic and neurite outgrowth activity. *Science* 1990;**250**(4988):1690–4.
47. Vanderwinden JM, Mailleux P, Schiffmann SN, Vanderhaeghen JJ. Cellular distribution of the new growth factor pleiotrophin (HB-GAM) mRNA in developing and adult rat tissues. *Anatomy and Embryology* 1992;**186**(4):387–406.
48. Wanaka A, Carroll SL, Milbrandt J. Developmentally regulated expression of pleiotrophin, a novel heparin binding growth factor, in the nervous system of the rat. *Brain Research Developmental Brain Research* 1993;**72**(1):133–44.
49. Silos-Santiago I, Yeh HJ, Gurrieri MA, Guillerman RP, Li YS, Wolf J, et al. Localization of pleiotrophin and its mRNA in subpopulations of neurons and their corresponding axonal tracts suggests important roles in neural-glial interactions during development and in maturity. *Journal of Neurobiology* 1996;**31**(3):283–96.
50. Deuel TF, Zhang N, Yeh HJ, Silos-Santiago I, Wang ZY. Pleiotrophin: a cytokine with diverse functions and a novel signaling pathway. *Archives of Biochemistry and Biophysics* 2002;**397**(2):162–71.
51. Hienola A, Pekkanen M, Raulo E, Vanttola P, Rauvala H. HB-GAM inhibits proliferation and enhances differentiation of neural stem cells. *Molecular and Cellular Neurosciences* 2004;**26**(1):75–88.
52. Amet LE, Lauri SE, Hienola A, Croll SD, Lu Y, Levorse JM, et al. Enhanced hippocampal long-term potentiation in mice lacking heparin-binding growth-associated molecule. *Molecular and Cellular Neurosciences* 2001;**17**(6):1014–24.
53. Pavlov I, Võikar V, Kaksonen M, Lauri SE, Hienola A, Taira T, et al. Role of heparin-binding growth-associated molecule (HB-GAM) in hippocampal LTP and spatial learning revealed by studies on over expressing and knockout mice. *Molecular and Cellular Neurosciences* 2002;**20**(2):330–42.
54. Perez-Pinera P, Alcantara S, Dimitrov T, Vega JA, Deuel TF. Pleiotrophin disrupts calcium-dependent homophilic cell–cell adhesion and initiates an epithelial-mesenchymal transition. *Proceedings of the National Academy of Sciences of the United States of America* 2006;**103**(47):17795–800.